https://doi.org/10.5194/egusphere-2025-2316
Preprint. Discussion started: 28 May 2025

Role of sea ice, stratification, and near-inertial oscillations in shaping the upper Siberian Arctic Ocean currents

Igor V. Polyakov[1], Andrey V. Pnyushkov[2], Eddy C. Carmack[3], Matthew Charette[4], Kyoung-Ho Cho[5], Steven Dykstra[6], Jari Haapala[7], Jinyoung Jung[5], Lauren Kipp[8], Eun Jin Yang[5]

1 International Arctic Research Center and College of Natural Science and Mathematics, University of Alaska Fairbanks, Fairbanks, 99775, USA
2 International Arctic Research Center, University of Alaska Fairbanks, Fairbanks, 99775, USA
3 Institute of Ocean Sciences, Fisheries and Oceans Canada, 9860 West Saanich Road, Sidney, BC, V8L 4B2, Canada
4 Woods Hole Oceanographic Institution, 266 Woods Hole Road, Woods Hole, Massachusetts, 02543, USA
5 Korea Polar Research Institute, Incheon, Korea
6 College of Fisheries and Ocean Sciences, University of Alaska Fairbanks, Fairbanks, USA
7 Finnish Meteorological Institute, Helsinki, Finland
8 Rowan University, 201 Mullica Hill Road, Glassboro, New Jersey, 08028, USA

Correspondence to: Igor V. Polyakov, 907-474-2686, ivpolyakov@alaska.edu

https://doi.org/10.5194/egusphere-2025-2316
Preprint. Discussion started: 28 May 2025

Abstract. The Siberian Arctic Ocean (SAO) is the largest integrator and redistributor of Siberian freshwater resources and acts to significantly influence the Arctic climate system. Moreover, the SAO is experiencing some of the most notable climate changes in the Arctic, and advection of anomalous Atlantic- (atlantification) and Pacific-origin (pacification) inflow waters and biota continue to play a major role in reshaping the SAO in recent decades. However, logistical challenges have limited our observation-based understanding of the upper SAO. In this study, we use a large collection of mooring data to create a coherent picture of the spatiotemporal patterns and variability of currents and shear in the upper SAO during the past decade. Although there was no noticeable trend in the upper SAO's current speed and shear from 2013 to 2023, their seasonal cycle has significantly strengthened. The cycle follows a coherence of upper ocean dynamics and sea ice state, as evidenced by the high correlation (–0.94) between seasonal cycles of sea ice concentration and current shear (less ice drives stronger currents and shear). In the shallow (<20-30m) summer surface mixed layer, currents have increased because strong stratification prevents wind energy from propagating into the deeper layers. In this case, strong near-inertial currents account for more than half of the summertime current speed and shear. In the winter, a thicker surface layer is created by deep upper SAO ventilation due to atlantification, which distributes wind energy to far deeper (>100m) layers. These findings are critical to understanding the ramifications for mixing and halocline weakening, as well as the rate of atlantification in the region.

1 Introduction

The Siberian Arctic Ocean (SAO), encompassing the Laptev and East Siberian seas and adjacent deep basins, plays a significant role in the Arctic climate system (**Fig. 1**). It is the Arctic Ocean's largest continental shelf system, and integrates Siberian freshwater inputs that account for over 10% of global river discharge. Moreover, the SAO is undergoing some of the most dramatic climatic changes in the Arctic (e.g., Polyakov et al., 2025a). Remote climate drivers, such as advection of anomalous Atlantic- (atlantification) and Pacific-origin (pacification) inflow waters and biota into the polar basins, have played a major role in reshaping the SAO. For instance, atlantification decreases stratification, enhances oceanic heat fluxes in the region, and has contributed to a decay of sea ice in the SAO over recent decades (Polyakov et al. 2023, 2025a). These physical changes have significant ecological consequences, including the arrival of new Pacific and Atlantic species in the East Siberian Sea (Ershova and Kosobokova, 2019).

https://doi.org/10.5194/egusphere-2025-2316
Preprint. Discussion started: 28 May 2025

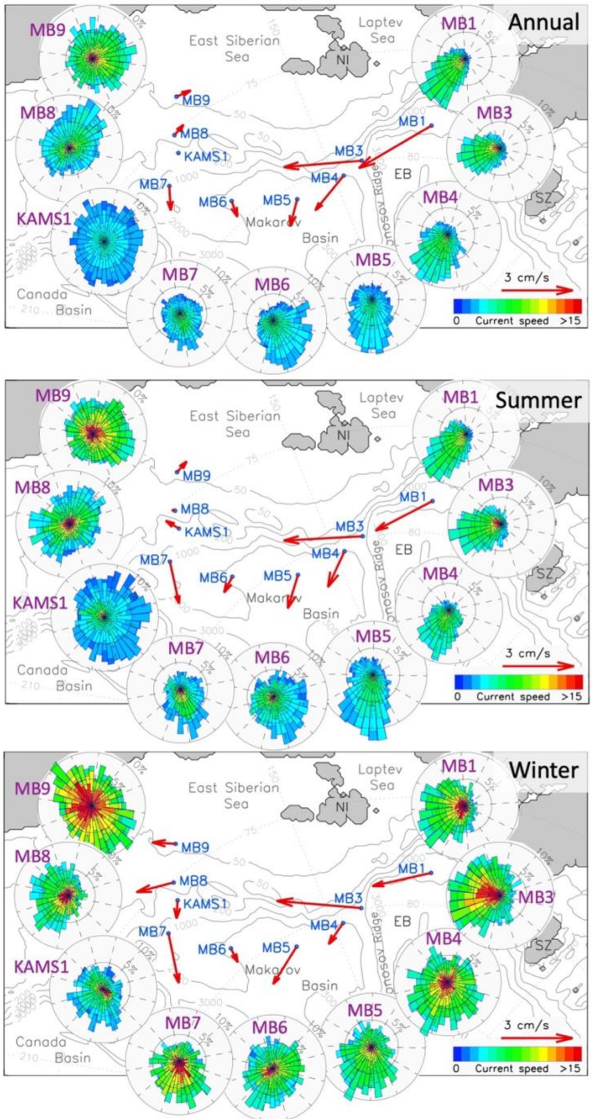

Figure 1. Annual, summer (J–S), and winter (N–A) 2021–2023 mean current vectors and roses of instantaneous (hourly) currents for a depth range of 10–30 m at nine mooring sites in the Siberian Arctic. The mooring positions are represented by the beginning of the red vectors. Roses are placed to indicate exact directions.

https://doi.org/10.5194/egusphere-2025-2316
Preprint. Discussion started: 28 May 2025

Despite evidence of fundamental changes, such as regional reduction of sea ice, disappearance of permanent halocline and altered freshwater transport across the SAO, quantification of many processes remains limited. At the same time, changes of upper ocean circulation in response to climate change are not well documented, and the interplay between mesoscale-to-seasonal events and long-term trends remains unclear. Particularly, the role of high-frequency processes acting at time scales of hours to days in rapidly changing SAO is not well understood whereas they are often the dominant components in time-series measurements of Arctic ice and ocean velocity variability [e.g., Plueddemann, 1992; Kwok et al., 2003; Rainville and Woodgate, 2009; Gimbert et al., 2012; Brenner et al. 2023]. These processes include semidiurnal tides and wind-forced near-inertial currents (NIC). Brenner et al. 2023 provide a good summary of near-inertial oscillations for further information. Details on the fundamentals of the mechanisms and drivers of the Arctic Ocean circulation can be found in (Timmermans and Marshall 2020). These knowledge gaps underscore the urgent need for in-depth analysis of the variability in the SAO currents at various time scales to better understand the dynamics and transformations of the SAO as it transitions to a new climatic state.

In this study, we build a cohesive picture of spatiotemporal patterns and variability of currents and shear in the upper SAO over the recent years using an extensive collection of mooring data. Shear plays a critical role in vertical mixing, stratification, and the distribution of heat and salt—processes that are especially important in the stratified and rapidly changing Arctic Ocean. Particularly, we map the time-dependent distribution of currents and their shear in the upper SAO; assess the role of sea ice, stratification, and NIC in setting the seasonal cycle of currents and shear in the region; and quantify the effect of winds on seasonal cycles of currents and shear in the surface mixed layer and halocline.

2 Data

Mooring observations: Our analysis utilizes the collection of instrumental observations of ocean currents from nine moorings distributed in the Siberian Arctic Ocean; see **Fig. 1** for locations. Moorings MB1 and MB3–MB9, maintained by the Nansen and Amundsen Basins Observational System (NABOS) program, were deployed from September 2021 through September 2023. Mooring KAMS1, maintained by the Korean Polar Research Institute (KOPRI), was deployed from August 2017 through September 2023. At the MB1 mooring site observations began in August 2002, thus providing invaluable long-term measurements which were used to place shorter 2021–2023 records in a longer context. All moorings used in this analysis provided current observations from upward-looking 300-kHz Acoustic Doppler Current Profilers (ADCP) for the upper 40-50m. ADCP records were complemented in this analysis by

https://doi.org/10.5194/egusphere-2025-2316
Preprint. Discussion started: 28 May 2025

profiles of currents from a McLane Moored Profiler (MMP) for the depth range of ~40-1000m at MB1. ADCPs provided current velocities, averaged over 2-m vertical cells, with at least 1-h time resolution. The manufacturer's estimates for 300-kHz ADCP accuracies are 0.5% of measured speed and 2° for current direction. The MMP sampled a vertical profile of water temperature, salinity, and current along the mooring line once per two days at a speed of ~25 cm/s with a sampling period of 0.5 s; therefore, the data had a vertical spacing of ~12 cm. According to the manufacturer's manual, an instrumental error of the acoustic current meter (ACM) installed at MMPs is ±0.5 cm

s^{-1}. The instrumental accuracy of the MMP magnetic compass is 2°. However, due to the weak horizontal component of the geomagnetic field in the Arctic Ocean, the individual compass error may exceed the instrumental accuracy, reaching 30° (Thurnherr et al., 2017).

Temperature-salinity ship-based observations: Ship-based summer (September-October) profiles of water temperature and salinity carried out in 2021 and 2023 complemented mooring observations, to provide CTD (conductivity-temperature-depth) measurements in the upper ~5–200m. CTD instruments have good vertical resolution and high accuracy of temperature (0.001°C) and salinity (0.003 psu) measurements.

Winds: Monthly 10-m winds during 1979–2023 used in this study are from the European Centre for Medium-Range Weather Forecasts reanalysis ERA-5, downloaded from https://cds.climate.copernicus.eu/cdsapp#!/home. The horizontal resolution of the data is 0.25°.

Sea ice concentrations: The Advanced Very High-Resolution Radiometer (AVHRR) satellite archive used in this study includes global daily sea ice concentration from 1981–2023 with 0.25x0.25° spatial resolution (https://www.ncdc.noaa.gov/oisst).

3 Methods

Defining buoyancy frequency (N): N is a measure of stability of a fluid. The mooring-based MMP measurements are used to quantify stratification using Brunt-Väisälä buoyancy frequency N, $N^2 = -(g/\rho_o)\partial\rho/\partial z$, where ρ is the potential density of seawater, ρ_o is the reference density (1030 kg m^{-3}), and g is the acceleration due to gravity. Increased fluid stratification (stability) is indicated by increased N.

Mean current speeds: The mean current speed, $|\mathbf{U}|$, for a specified time interval is obtained as the time average of instantaneous speeds, $|\mathbf{U}| = (u(t)^2+v(t)^2)^{1/2}$, where u and v are the east and north components of

https://doi.org/10.5194/egusphere-2025-2316
Preprint. Discussion started: 28 May 2025

either the total, measured current or the semidiurnal (near-inertial) band-passed current (see next paragraph).

Vertical shear of horizontal currents: The vertical shear utilizing ADCP and MMP current observations was calculated using the central finite difference method (when the shear at a vertical grid point is proportional to the difference between the velocities of two nearby, shallower and deeper, grid points), which produced a 4 m vertical scale for the shear estimates.

Estimating semidiurnal-band (near-inertial) and residual currents: Near-inertial currents were estimated using hourly current zonal and meridional components that were band-pass filtered between 10- and 14-hour periods. The result of this procedure is referred to as NIC in the text. Residual currents are the result of subtracting NIC from the original current records.

Separating tidal and inertial oscillations: In the SAO, the semi-diurnal ocean currents comprise both tidal and near-inertial components. Separating contributions from the closely spaced M_2 and S_2 tidal constituents, along with near-inertial waves, to the current variability at semidiurnal time scales is challenging due to their frequency proximity and the low signal-to-noise ratio in central Arctic mooring velocity records. Previous studies (e.g., Pnyushkov and Polyakov, 2012; Baumann et al. 2020, 2022) relied on conventional harmonic analysis, which struggles with contamination from non-stationary near-inertial waves, potentially inflating tidal harmonic amplitudes during the ice-free season. In this study, we used a novel method to separate tidal and near-inertial amplitudes using different window widths for tidal and near-inertial oscillations. The basic idea is that although wind-generated NIC have a synoptic timescale, tidal currents may be consistently measured over a 30-day timescale using hourly observations. In this analysis, we used a significantly shorter 2-day window for NIC detection.

An example of application of this technique to the 2021–2023 MB1 mooring data is shown in **Fig. S1**. In the upper 35m of the SAO inertial currents are the dominant constituent of semidiurnal currents, with a mean amplitude of 3.8 cm/s—approximately twice as strong as the M_2 tidal current (1.9 cm/s). The mean amplitude of the second most energetic tidal constituent, S_2, is 0.3 cm/s. NIC exhibit strong seasonal variability. From November to June, NIC amplitudes (~2 cm/s) are comparable to tidal currents, but from June through September, as sea ice retreats, NIC intensify sharply, peaking at 13 cm/s in September 2023.

This short note is provided here to help in the interpretation of the near-inertial signal in the current data, which indicates that the SAO NIC is dominated over the summer by inertial currents rather than tidal constituents. Another paper will examine inertial and tidal semi-diurnal currents in greater detail.

https://doi.org/10.5194/egusphere-2025-2316
Preprint. Discussion started: 28 May 2025

4 Results

4.1 Documenting currents and shear in the upper Siberian Arctic Ocean in 2021–2023

The average currents for the upper 30m of the Siberian Arctic during a two-year period (September 2021 – September 2023) are shown in **Fig. 1**. Strong topographic steering causes currents in the outer western SAO (Eurasian Basin, MB1 and MB3 mooring records) to be along-slope even in the very top layer, supporting a previous finding by Pnyushkov et al. (2021). This SAO region has the strongest (up to 3 cm/s) mean currents, which do not vary greatly from season to season (**Fig. 1**). In the central SAO (moorings MB4–MB7), the currents become weaker (1-2 cm/s) and gentler slopes reduce topographic steering, and currents acquire a greater off-shore northward component, forming the origin of the Transpolar Drift (Kipp et al. 2023). The mean currents (vectors in **Fig. 1**) on the shelf are weak because they lack a dominant direction, even if the instantaneous currents are typically greater, particularly in summer (as indicated by the red color of current roses). From 2021 to 2023, the East Siberian Sea shelf also shows a divergent pattern of seasonal currents, with winter currents predominantly flowing eastward (to the left according to the map orientation) and summer currents flowing westward.

The hourly mooring records of total current speed |**U**| and shear ($\mathbf{U_z}$) in the upper 30m layer are shown in **Fig. 2**. The largest currents and shear correspond to the ice-free season in all mooring records, consistent with previous observations showing that compact sea ice cover dampens the ocean response to wind forcing (Lenn et al., 2011; Lincoln et al., 2016; Rainville and Woodgate, 2009; Polyakov et al. 2020a). The spatiotemporal patterns of total and near-inertial currents and their shear during these two years are very similar, suggesting that the near-inertial currents play a key role in determining the dynamics of the upper ocean in the SAO (**Fig. 3**). Annually and seasonally averaged total and near-inertial currents and their shear in the central SAO are shown in (**Fig. 4**). This figure provides further evidence that near-inertial currents contribute significantly to both total current speed and shear (on average 54% and 40%, respectively). This contribution is particularly significant in the summer, when, on average, the near-inertial component explained 64% (50%) of the total current speed (shear) in eight mooring records. This ratio was remarkably stable, geographically varying from only 69% (53%) for the annual records at the MB1 mooring site to 61% (56%) at MB9.

The annual and seasonal total and near-inertial currents were generally weaker in the central SAO than those in more eastern and western regions (**Fig. 4a-c**). For example, the total annual |**U**| minimum of ~ 4cm/s is found at the MB5 mooring location. Although the spatial pattern of shear is noisier, the MB5 mooring record still tends to show the weakest shear. At all SAO mooring locations, the shear in the upper 30m is significantly increased throughout the summer.

https://doi.org/10.5194/egusphere-2025-2316
Preprint. Discussion started: 28 May 2025

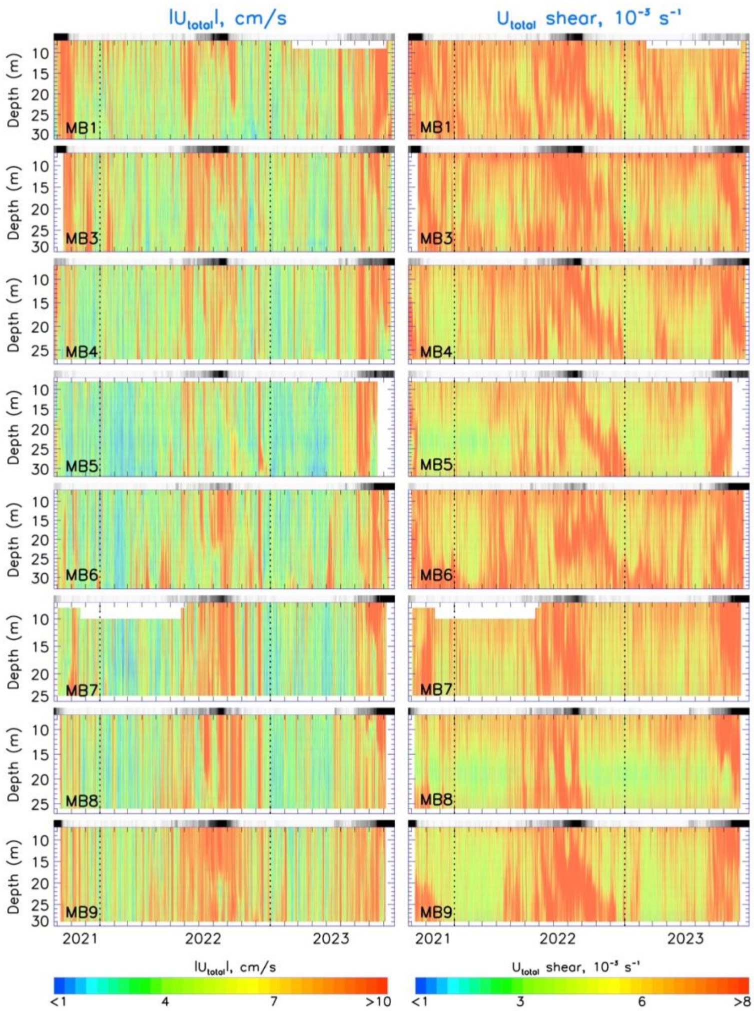

Figure 2: Biennial (September 2021 – September 2023) records, showing the magnitude of the total currents (left) and associated shear (right) at eight NABOS mooring locations (see **Fig. 1**) as a function of time and depth. White segments show missing data. Black-grey-white bar over each panel shows daily sea ice concentration between 0% (black indicating ice-free summer) to 100% (white indicating winter), with near grey scale for interseasonal transitions. Vertical dotted lines show transitions from year to year. Note that there are minor variations in the vertical data coverage of the mooring records.

https://doi.org/10.5194/egusphere-2025-2316
Preprint. Discussion started: 28 May 2025

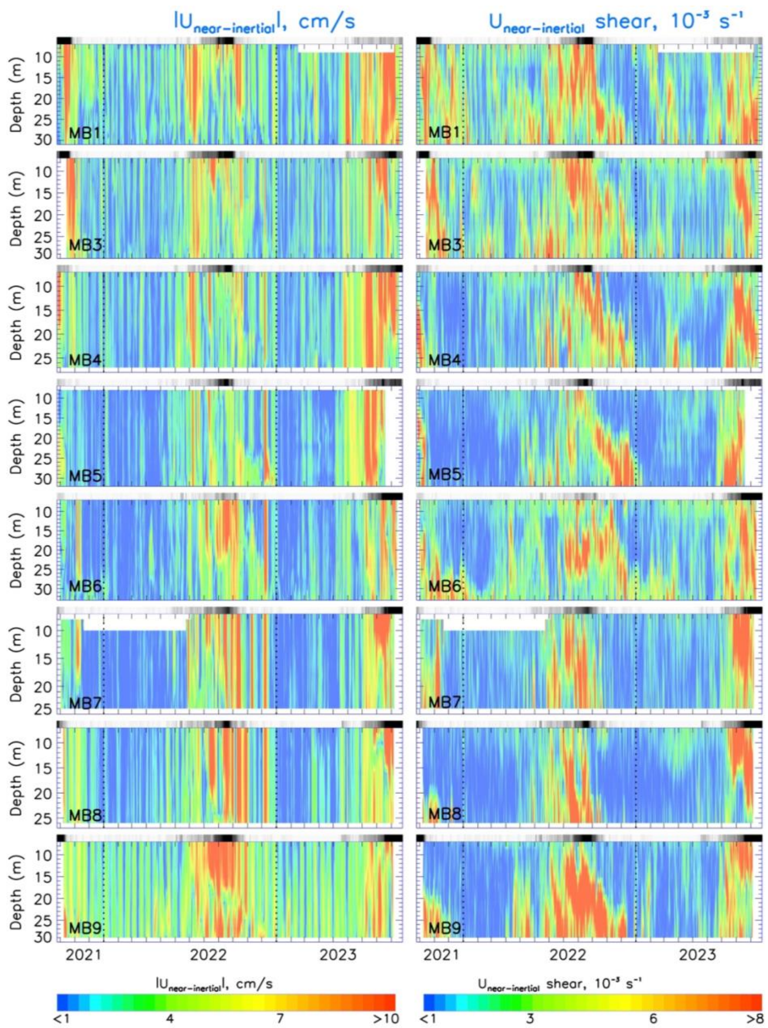

Figure 3: Biennial (September 2021– September 2023) records, showing the magnitude of the semidiurnal-band (near-inertial) currents (left) and associated shear (right) at eight NABOS mooring locations (see **Fig. 1**) as a function of time and depth. White segments show missing data. Black-grey-white bar over each panel shows daily sea ice concentration between 0% (black indicating ice-free summer) to 100% (white indicating winter), with near grey scale for interseasonal transitions. Vertical dotted lines show transitions from year to year. Note that there are minor variations in the vertical data coverage of the mooring records.

https://doi.org/10.5194/egusphere-2025-2316
Preprint. Discussion started: 28 May 2025

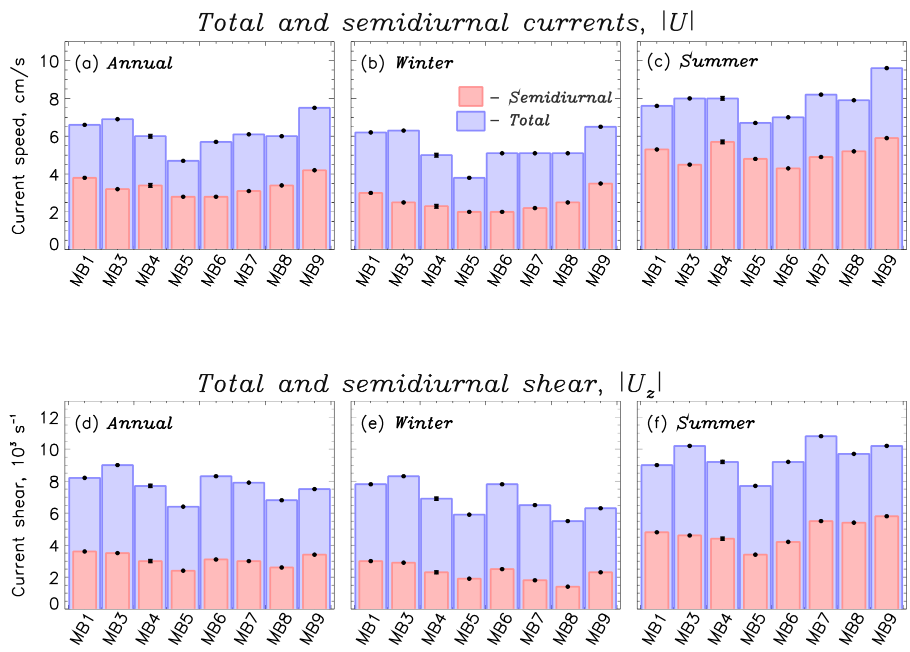

Figure 4: Temporal changes in total (blue) and semidiurnal-band (near-inertial, red) currents and their shear from September 2021 to September 2023 in the upper 30 m for eight locations in the Siberian Arctic. Estimates of (a, d) annual (January – December), (b, e) winter (November-July), and (c, f) summer (August-October) for mean current speed |**U**| and vertical shear of horizontal currents |$\mathbf{U}_z$| respectively, at eight mooring locations. Statistical significance of means (error bars) is shown at the 95% confidence level.

4.2 Variability of currents and shear in the upper SAO

4.2.1 Seasonal variability in the upper SAO

The seasonal signal is the dominant component of Arctic atmospheric, sea ice, and oceanic variability (e.g., Polyakov et al. 2025b). The winter winds, which are typically stronger than the summer winds (**Fig. 5**), should be the primary cause of this variability in the upper ocean currents. Indeed, surface-intensified upper ocean currents provide evidence that the atmospheric forcing dominates (**Fig. 2**). At the same time, the ocean's response to this seasonal forcing is not straightforward due to a host of mechanisms and

https://doi.org/10.5194/egusphere-2025-2316
Preprint. Discussion started: 28 May 2025

processes involved. For example, summer currents, not winter ones, are stronger in the upper 30m SAO due to (at least partially) the isolating effect of compact winter sea ice (**Figs. 2-4** and **6**).

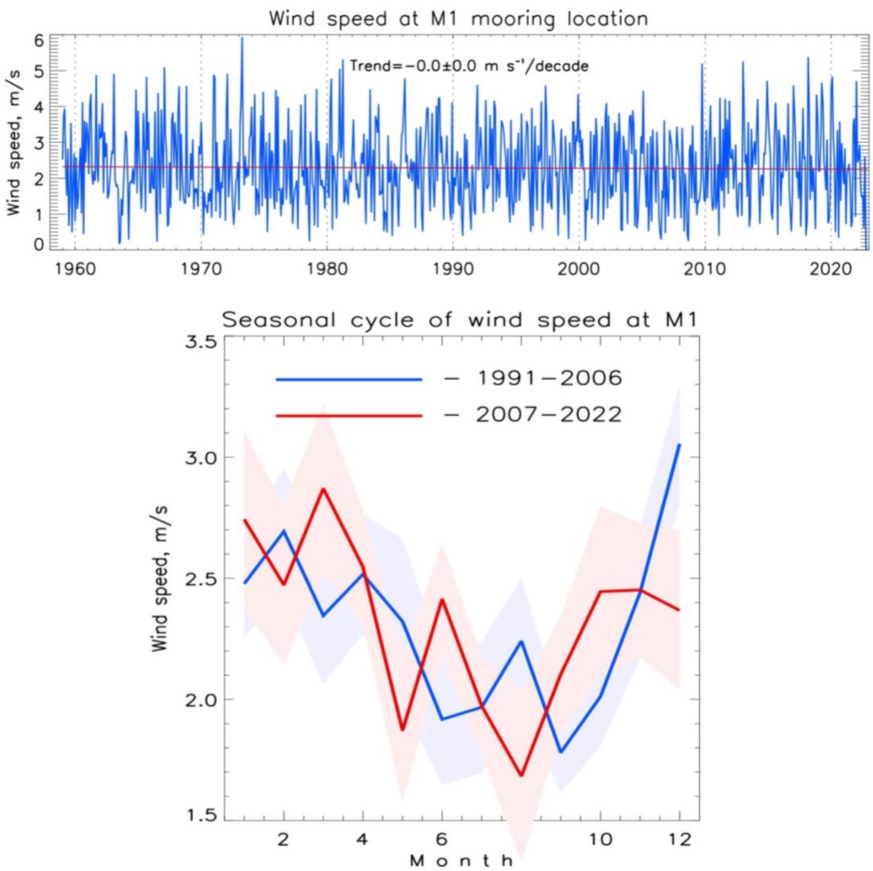

Figure 5: (Top) 1958 –2023 time series of wind speed from monthly ERA-5 reanalysis for the M1 mooring location. (Bottom) Seasonal cycle of wind speed at the MB1 mooring location averaged over 1991–2006 (blue) and 2007–2022 (red). Shades represent 1 S.E. uncertainty. Note negligible trend and statistically insignificant temporal changes in seasonal cycles.

https://doi.org/10.5194/egusphere-2025-2316
Preprint. Discussion started: 28 May 2025

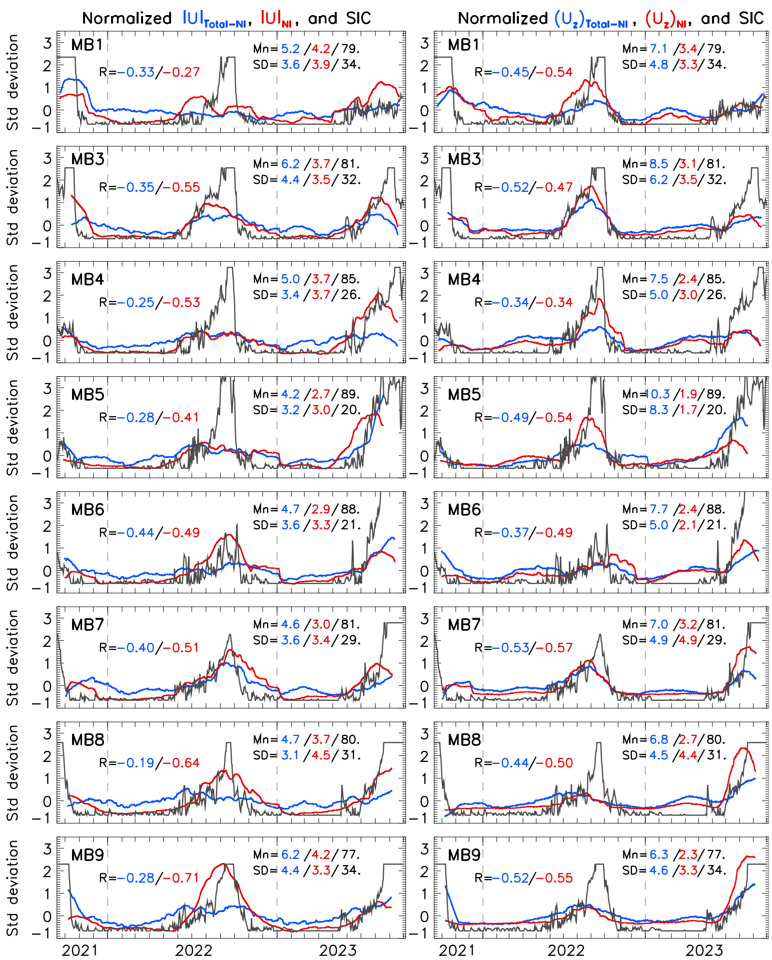

Figure 6: Time series of normalized (reduced to anomalies by subtracting means, Mn, and divided by standard deviations, SD) current speed |**U**|, vertical shear of horizontal current $\mathbf{U}_z$ (both from 10m depth level), and sea ice concentration SIC (the latter time series are multiplied by minus one) at eight mooring locations. Blue lines show parameters for total minus near-inertial currents, red lines show parameters for near-inertial currents, and gray lines show SIC. Mn and SD are provided for |**U**| in cm/s, $\mathbf{U}_z$ in 10^3 s^{-1} and SIC in %. Correlations R between |**U**| and SIC (blue digits) and $\mathbf{U}_z$ and SIC (red digits) are all statistically significant at 0.05% level.

https://doi.org/10.5194/egusphere-2025-2316
Preprint. Discussion started: 28 May 2025

The connectivity between the sea ice state (expressed by its concentration) and the SAO's |**U**| and $\mathbf{U_z}$ is evident in **Fig. 6**, which shows an increase in currents and shear in the upper ocean (10m depth) in the summer following a decrease in sea ice concentration. In that, the start and end of summer intensification of |**U**| and, in particular, $\mathbf{U_z}$ at all SAO mooring sites closely follows the early summer sea ice decay and start of freezing in fall. This relationship is evident from the statistically significant correlations between the time series of sea ice concentration from one side and current speed and shear from the other side (**Fig. 6**). The correlation analysis shows that sea ice concentration and shear are more closely related than current speed, and that sea ice concentration is more strongly correlated with near-inertial currents than with residual (total minus near-inertial) currents. There is no obvious regional bias toward higher or lower correlation in the SAO. Seasonal cycles of sea ice concentration, |**U**|, and $\mathbf{U_z}$ averaged over longer (2013–2023) records from the MB1 mooring location further and more strongly corroborate this precise tuning of upper ocean dynamics and sea ice state (**Fig. 7a,b**).

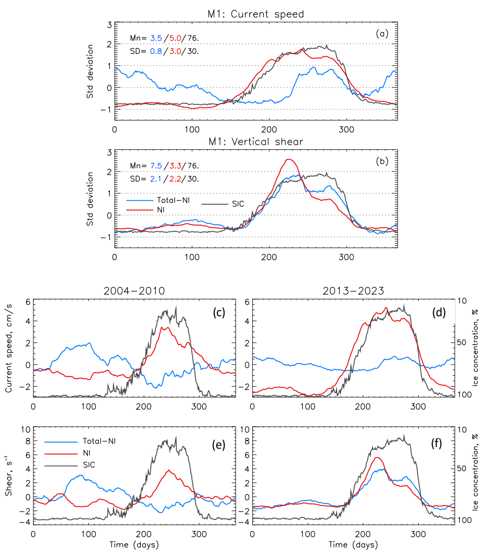

Figure 7: (a,b) Mean 2013–2023 seasonal cycle of current speed (|**U**|, cm/s, blue), vertical shear of horizontal current ($\mathbf{U_z}$, 10^3 s^{-1}, red), and sea ice concentration (SIC, %, grey, multiplied by minus one) reduced to anomalies by subtracting means (Mn) and normalized by standard deviations (SD). (c-f) Mean 2004–2010 and 2013–2023 seasonal cycles of current speed (|**U**|, cm/s, blue), vertical shear of horizontal current ($\mathbf{U_z}$, 10^3 s^{-1}, red), and sea ice concentration (SIC, %, grey). 10m depth at MB1 mooring location (eastern Eurasian Basin). Monthly running mean smoothing is applied to all time series.

https://doi.org/10.5194/egusphere-2025-2316
Preprint. Discussion started: 28 May 2025

4.2.2 Longer-term variability in the upper western SAO

Before discussing decadal-scale changes in stratification and currents in the SAO, we note that regional wind speeds have not increased, nor has the seasonal cycle of wind undergone any statistically significant shift since the 1990s (**Fig. 5**). Therefore, other factors like sea ice and ocean stratification controlled the observed changes. In this analysis, decadal (2004–2023) records of total and near-inertial currents and shear from the MB1 mooring are used to validate results based on shorter 2021–2023 records and to provide further insight into interannual variability in the SAO.

The seasonal pattern of currents and shear in the upper 30m seen in MB1 2013–2023 mooring record (**Fig. 8**) is comparable to our results utilizing mooring records from eight distributed mooring locations in the SAO (**Figs. 2, 3**). In that, the strength of currents and the magnitude of shear observed in the eastern Eurasian Basin (MB1 mooring) in 2021–2023 (both annual and seasonal, total and near-inertial) were similar (e.g., compare the annual mean current speed of 7.3 and 6.8 cm/s averaged across 2013–2020 and 2021–2023, respectively), **Fig. 9**. Throughout this decade, there was no apparent rising or decreasing trend in the current speed and shear of the upper ocean. Overall, the currents and shear were stronger than those seen from 2004 to 2009, notwithstanding some discernible interannual changes, especially during the summer (**Fig. 9**).

The late 2015–early 2018 period stands out due to its decreased currents and shear in every season. During this period, anomalously fresh water was advected from the Kara Sea through the Vilkitsky Strait (owing to amplified discharge from the Enisey River), causing a major freshening of the upper eastern Eurasian Basin (More and Polyakov 2025). Strong stratification in the area had a profound effect on upper ocean dynamics and restricted upward heat fluxes from the ocean interior (see Fig. 4 from Polyakov et al. 2020b). This may explain why throughout the summer months of these years, sea ice has been present in the area, but during the summer months of the previous and following years, there was none at all (**Fig. 10**).

https://doi.org/10.5194/egusphere-2025-2316
Preprint. Discussion started: 28 May 2025

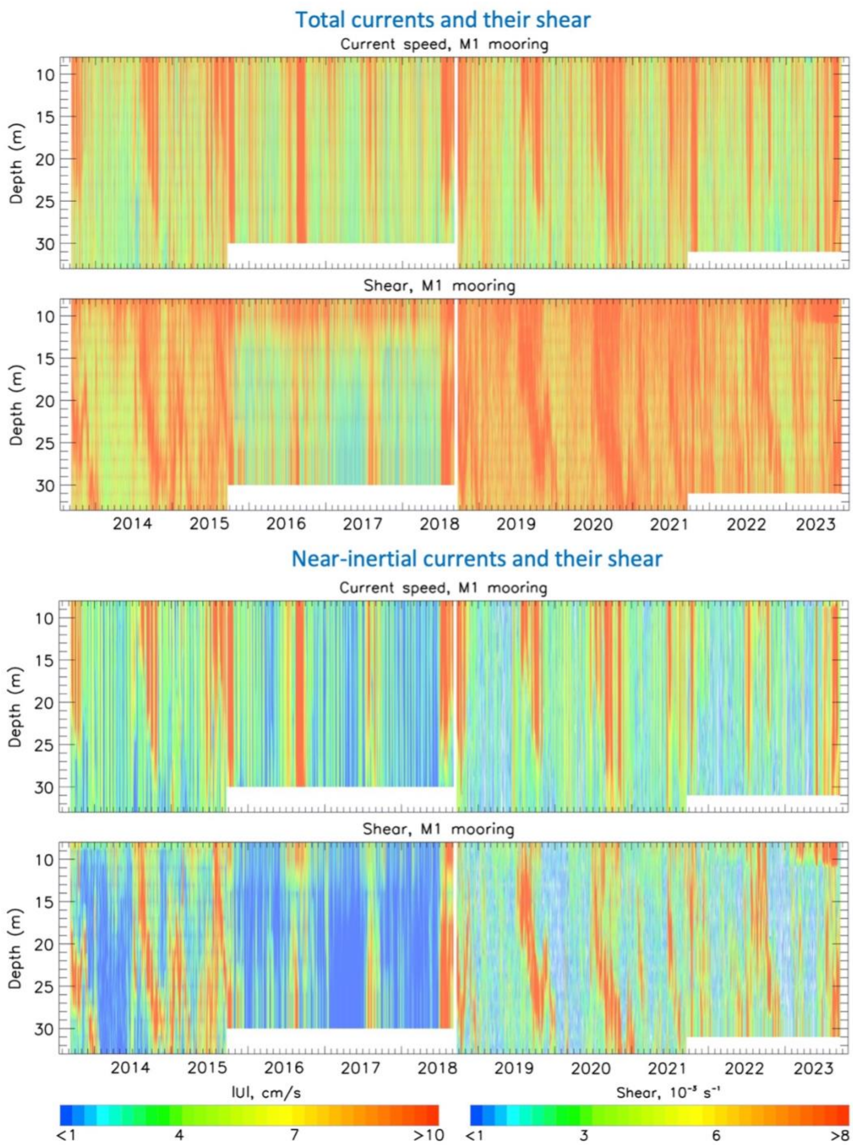

Figure 8: September 2013 – September 2023 record of the total and semidiurnal-band (near-inertial) current speed (cm/s) and associated shear (10^3 s^{-1}) at MB1 mooring location (see **Fig. 1** for mooring position) as a function of time and depth. White segments show missing data.

https://doi.org/10.5194/egusphere-2025-2316
Preprint. Discussion started: 28 May 2025

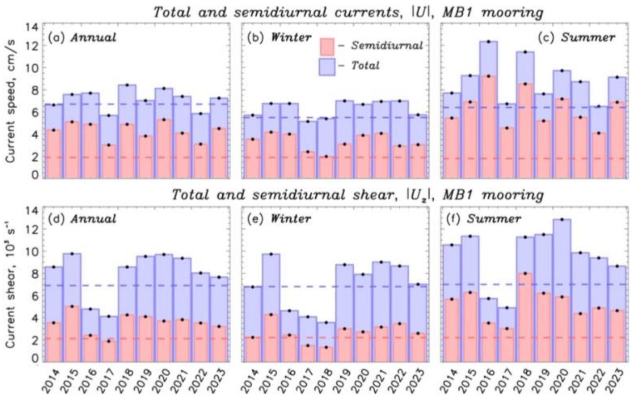

Figure 9: Temporal changes in total (blue) and semidiurnal-band (near-inertial, red) currents and their shear from 2014 to 2023 in the upper 30 m. Estimates of (a, d) annual (January – December), (b, e) winter (November-July), and (c, f) summer (August-October) for mean current speed |**U**| and vertical shear of horizontal currents $|\mathbf{U}_z|$ respectively, at M1 mooring location. Dashed blue and red horizontal lines indicate 2004 –2009 means. Statistical significance of means (error bars) is shown at the 95% confidence level.

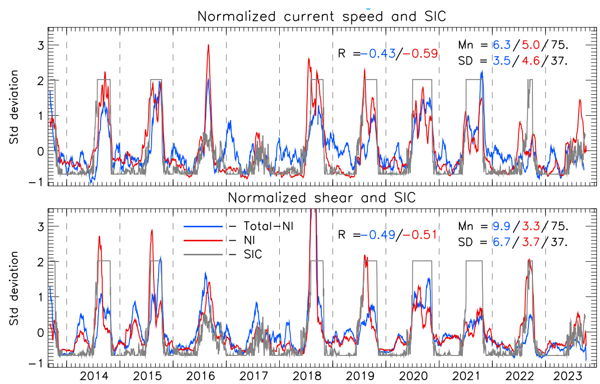

Figure 10: Time series of normalized (reduced to anomalies by subtracting means, Mn, and divided by standard deviations, SD) current speed |**U**|, vertical shear of horizontal current $|\mathbf{U}_z|$ (both from 10m depth level), and sea ice concentration SIC (the latter time series are multiplied by minus one) at M1 mooring location. Blue lines show parameters for total minus near-inertial currents, red lines show parameters for near-inertial currents, and gray lines show SIC. Mn and SD are provided for |**U**| in cm/s, $|\mathbf{U}_z|$ in 10^3 s^{-1} and SIC in %. Correlations *R* between |**U**| and SIC (blue digits) and $|\mathbf{U}_z|$ and SIC (red digits) are all statistically significant at 0.05% level.

https://doi.org/10.5194/egusphere-2025-2316
Preprint. Discussion started: 28 May 2025

A close examination of the eastern Eurasian Basin's decadal records of sea ice concentration, shear, and current speed reveals that the seasonal cycle has changed throughout time. In particular, summers associated with reduced sea ice concentration appear to have been longer in recent years across this decadal record, and the seasonal pattern of near-inertial and total currents has changed accordingly (**Fig. 10**). To place these changes in an even longer timeframe, we compare MB1 mooring records starting in 2004 to investigate the evolution of the seasonal cycle of SIC, $|\boldsymbol{U}|$ and $\boldsymbol{U}_z$ (**Fig. 7c-f**). The original current records from 2004 to 2010 used in our analysis are shown in Fig. 4 from Polyakov et al. 2020a.

When comparing seasonal cycles of SIC, $|\boldsymbol{U}|$ and $\boldsymbol{U}_z$ averaged over 2004–2010 and 2013–2023, a distinct and obvious tendency is the extension of the summer season for both sea ice concentration and currents. For example, the 80% SIC-defined winter-summer transition now occurs 20 days later in the fall and six days earlier in the spring (**Fig. 7c-f**). This is consistent with the findings by Stroeve and Notz (2018) and Polyakov et al. (2025b) which showed that in recent decades surface melt onset happens earlier and the freeze-up later. The currents and shear closely follow these seasonal changes in SIC. In the eastern Eurasian Basin, Polyakov et al. 2020a found an increasing coupling between the vertical shear of oceanic currents, wind, and ice from 2004 to 2018, particularly during the summer. Extending this record by additional five years, we corroborate these earlier results. Specifically, we show a strengthening of the seasonal cycle of $|\mathbf{U}|$ and $\mathbf{U_z}$ (expressed by greater summer/winter differences) and an enhanced negative correlation R between SIC and current strength and shear (less ice drives stronger current and shear). For example, the correlation between SIC and shear was $R = –0.73$ from 2004 to 2010, and an astounding $R = –0.94$ from 2013 to 2023. In the early period, but not in the more recent decade, the mean currents and shear in the upper 30m of the SAO follow the seasonal pattern of wind (in reaction to increased winter winds by enhanced winter currents). This is important for the following discussion.

4.3 Role of stratification

The depth of the surface mixed layer in the Arctic varies seasonally, thickening in winter (~25 to >50 m) and shallowing in summer (~5–30 m), and regionally, with a deeper layer in the Eurasian Basin, (~20 m in summer, ~70 to 100+ m in winter) than in Amerasian Basin (~8 m in summer, 30 m in winter) (Peralta-Ferriz and Woodgate 2015). Since SAO moorings lack temperature and salinity observations in the very top 20m layer, summer 2021 and 2023 CTD ship-borne snapshot observations and closest-in-time mooring-based profiles of $|\mathbf{U}|$ and $\mathbf{U_z}$ were used to demonstrate that the structure (stratification) of the surface mixed layer directly affects the upper ocean currents and their shear. Regardless of the depth of the mooring site, we find stronger currents in the surface layer that is bounded by significant density

https://doi.org/10.5194/egusphere-2025-2316
Preprint. Discussion started: 28 May 2025

gradients, while the maximum shear is linked to the base of this layer (**Fig. 11**). This analysis contributes to a better understanding of the seasonal evolution of the monthly profiles of currents and shear (both total and near-inertial), particularly the maximum of |**U**| and $\mathbf{U}_z$ as a signature of summer stratification in the upper 30m layer (**Fig. 12**). Eleven years of mooring observations were used to map the mean seasonal cycle of currents and associated shear in the upper 34m of the eastern Eurasian Basin (MB1 mooring). Their distinctive summer pattern may be understood as a stratification indicator (**Fig. 13a-c**).

The strong stratification-based bounding of upper ocean summer currents can be explained by the shallow water theory, which holds that the intensity of depth-averaged currents is proportional to wind stress and inversely proportional to layer thickness (~~Gelfenbaum & Stumpf, 1993~~). Thus, thinner layers have a higher concentration of wind energy and stronger currents. Is it therefore correct to state that wintertime deep ocean ventilation creates a much thicker surface layer, and that wind energy (which is higher in winter than in summer) is just dispersed over this thicker layer, resulting in a lack of strong currents in the upper 30m ocean that is caused by not just the screening effects of sea ice but also by very different stratification?

This interpretation is supported by observations in **Fig. 13e-j**, which show total, near-inertial, and residual (total minus near-inertial) seasonal mean currents from 2013–2023 MB1 mooring records, averaging across 10-110m depth at 20m intervals. Expectedly, increased currents, dominated by the near-inertial component, are observed in the stratified upper 10-30 m layer in summer. Deeper (>30m) depths present a different picture with a discernible rise in total and residual |**U**| in the winter (not near-inertial component) but no amplification of currents in the summer. A near-inertial component causes the summer maxima in vertically averaged total currents, while stronger winter winds, which transfer energy through residual currents over a deeper winter ventilated layer (including a part of halocline), create the winter maxima. Therefore, throughout the year, stratification plays a critical role affecting currents in the upper ocean. Moreover, stratification is strongly connected to sea ice, and in the observed tight connection between the seasonal evolution of currents and sea ice concentration (discussed in section 4.2a) stratification may be a physically significant intermediary link.

https://doi.org/10.5194/egusphere-2025-2316
Preprint. Discussion started: 28 May 2025

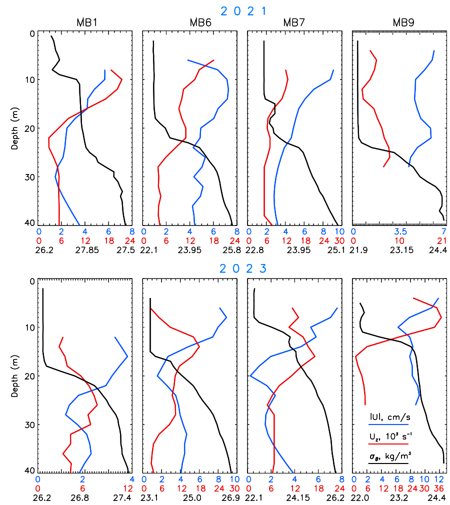

Figure 11: September snapshot vertical profiles of water density (black) from CTD cast and current speed (blue) and vertical shear of horizontal current (red) based on mooring ADCP observations. The ADCP records are selected based on their temporal proximity to the shipborne CTD casts (typically less than a day apart). Stratification has a clear impact on current speed and shear.

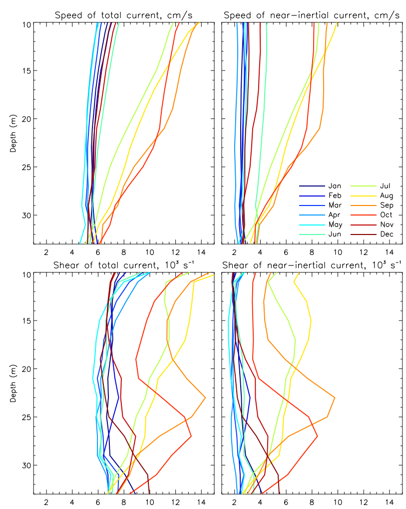

Figure 12: Monthly mean 2013–2023 vertical profiles of (top) current speed and (bottom) vertical shear of horizontal currents. Total current speed and shear are shown in the left column, while semidiurnal (near-inertial) current speed and shear are shown in the right. All data are from the MB1 eastern Eurasian Basin mooring.

https://doi.org/10.5194/egusphere-2025-2316
Preprint. Discussion started: 28 May 2025

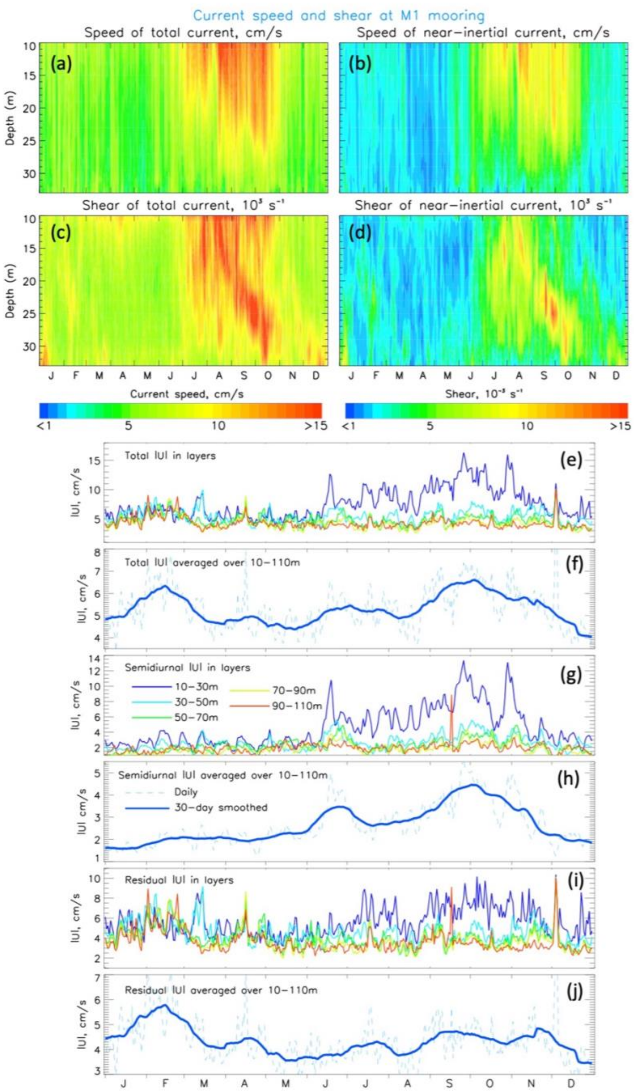

Figure 13: (a-d) Mean 2013–2023 seasonal cycle of current speed (a,b) and vertical shear of horizontal current (c,d) of total (a,c) and semidiurnal (near-inertial, b,d) currents. (e,f) Mean 2018–2021 current speed averaged within 20m depth intervals (e) and over a 10 –110m depth range (f). (g,h and i,j) Same as in (e,f) but for semidiurnal (g,h) and residual (total minus semidiurnal, i,j) currents. All data are from MB1 eastern Eurasian Basin mooring.

https://doi.org/10.5194/egusphere-2025-2316
Preprint. Discussion started: 28 May 2025

Figure 14 which shows the 2021–2023 mooring records from the upper 45-200m layer of the eastern Eurasian Basin, is used to illustrate the points in the preceding paragraph. These profiler-based observations have a rather coarse (two-day) temporal resolution and cannot resolve near-inertial currents. However, they combine a relatively high vertical resolution of temperature, salinity, and currents, and they show seasonal development of ventilation, as seen by the deepening of the maximum buoyancy from December-January into late winter. These records show how the upper 100–120m stratification decreases in the winter, allowing wind energy to enter deeply and causing greater currents and late-winter shear.

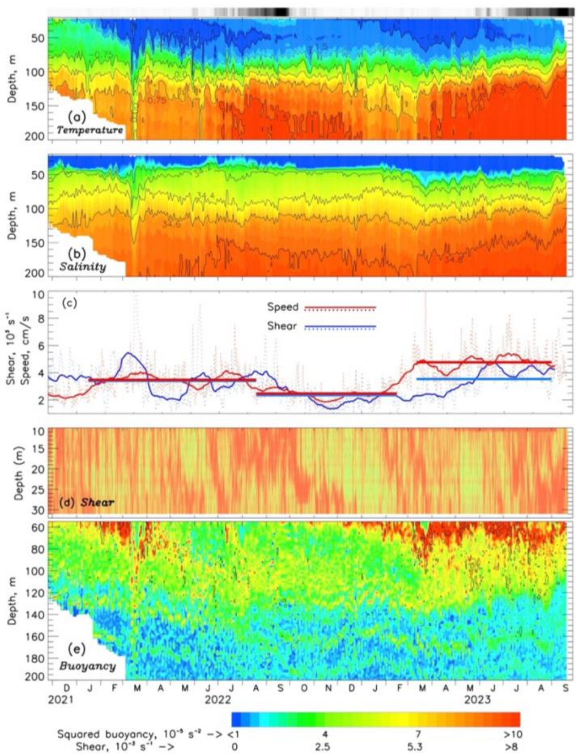

Figure 14: (a) Potential temperature (ºC), (b) salinity, (c) current speed and shear averaged over 50-140m depth range (dashed lines are daily values and solid lines are monthly means, horizontal segments show long-term means), (d) current shear (10^{-3} s^{-1}), and (e) squared buoyancy frequency (10^{5} s^{-2}); thin black lines show 0.9×10^{3} s^{-1} shear as an indicator of high winter shear in the upper 200m of the eastern Eurasian Basin (MB1 mooring location) in 2021-2023. Black-gray-white bar over the top panel shows daily sea ice concentration between 0% (black) and 100% (white) with linear color scale in between. White segments show missing data.

https://doi.org/10.5194/egusphere-2025-2316
Preprint. Discussion started: 28 May 2025

Further evidence of the critical role ocean stratification plays in redistributing wind energy with depth can be found in **Fig. 7c,e**, which shows the presence of winter maximum of mean ocean current speed in the upper 30m layer due to stronger stratification and shallower mixed layer in 2004–2010, when ventilation in the upper Eurasian Basin was not that deep and stratification was stronger (Polyakov et al. 2017, 2020b).

5 Discussion

Mooring observations provided solid observational evidence that, predominantly wind driven, the upper ocean circulation in the SAO accumulates and converges flows of shelf freshwater from east and west in the East Siberian Sea, thereby acting as an integrator of river discharge (e.g., Jones 2001, Armitage et al., 2017). Cross-slope water and biogeochemical exchanges (e.g., Bauch et al. 2014), in contrast, are suppressed in the western SAO (Eurasian Basin) due to the constraining influence of strong topographic steering, such that flow, even in the very top layer, is aligned with the underlying topography regardless of wind direction (e.g., Pnyushkov et al. 2018). The mean currents in the western SAO region are the strongest, reaching up to 3 cm/s, and they vary little from season to season. Cross-shelf exchange is elevated east of the Lomonosov Ridge, where slope angles are relaxed. In this area, the currents become weaker (1-2 cm/s) and acquire a greater off-shore northward component, forming the origin of the Transpolar Drift. This freshwater pathway is confirmed by geochemical tracers such as radium-228, and high fractions of meteoric water (Kipp et al., 2023; Charette et al., 2020). Averaged over 2021–2023, the mean currents on the shelf are small because they lack a preferred direction, even if the instantaneous currents are typically greater than in the deeper ocean, particularly in summer.

Throughout 2013–2023, there was no apparent trend in the current speed and shear in the upper western SAO. However, the $|\mathbf{U}|$ and $\mathbf{U}_z$ were stronger over this recent decade than those seen from 2004 to 2009. This pattern of temporal variability may be connected to the alternating decadal-scale atmospheric variability (Polyakov et al. 2023). However, throughout the last decade the seasonal cycle of sea ice concentration, shear, and current speed has changed in the upper SAO significantly. In particular, summers have been longer in recent years, causing surface melt to start earlier and freeze-up to happen later. This strengthened the seasonal cycle of $|\mathbf{U}|$ and $\mathbf{U}_z$ (expressed by greater summer/winter differences) and caused a precise tuning of upper ocean dynamics and sea ice state, as evidenced by a high correlation of $R = -0.94$ between SIC and current shear from 2013 to 2023 (less ice drives stronger currents and shear).

https://doi.org/10.5194/egusphere-2025-2316
Preprint. Discussion started: 28 May 2025

We found that currents in the halocline and surface layer are significantly impacted by the seasonal evolution of stratification. In the shallow (<20-30m) summer surface mixed layer, currents are increased because strong stratification constrains wind energy from propagating into the deeper layers. Strong wind-generated inertial currents that are generated when sea ice is reduced account for more than half of the summertime current speed and shear. Published measurements of ocean turbulence indicate that high-frequency (like near-inertial and tidal) processes can dominate time-averaged mixing rates and diapycnal fluxes (Padman and Dillon, 1991; D'Asaro and Morison, 1992; Padman, 1995; Crawford et al., 1999; Fer, 2014). In the winter, a thicker surface layer is created by deep upper SAO ventilation associated with atlantification, which distributes wind energy to far deeper (>100m) layers. We provide evidence of winter amplification in the average currents across the 100m upper ocean layer in response to higher wintertime wind forcing. This is highly consistent with increasing seasonality and a general loss of double-diffusive staircases in the region over the 2004 to 2023 period (Lundberg and Polyakov 2025). Consequently, stratification represents a physically significant link in the strong connection between the seasonal evolution of currents and sea ice concentration. This is consistent with findings of Brenner et al. (2023), who used a slab model results verified by mooring observations in the Beaufort Sea to show that both internal ice stresses and upper ocean stratification contribute to the intensity of inertial surface currents. Thus, while there has been no appreciable change in regional wind speed since the 1990s, sea ice and ocean stratification have been responsible for the observed changes in the upper SAO dynamics over the last few decades.

This analysis provides important insights on the consequences of ongoing atlantification of the SAO. For example, our finding of the dominant role of inertial currents in summer upper ocean dynamics is critical for developing reliable mixing schemes for climate models. This would improve the model performance making the simulated future eastward progression of atlantification more certain. The identification of deep propagation of wind forcing in winter into the SAO interior is critical to understanding the ramifications for mixing and halocline weakening, as well as the rate of atlantification in the region. There are still numerous questions about the future of the atlantification and its impact on the short- and long-term physical, geochemical, and biological responses in the SAO and at pan-Arctic scales. As our mooring data demonstrate, extreme freshening of the upper ocean between 2015 and 2017 can in fact slow down the rate of atlantification. This is consistent with studies demonstrating that the recent freshening in the upper Canada Basin has enhanced the stratification regionally (e.g., Carmack et al. 2016, Proshutinsky et al. 2019, Timmermans et al. 2023, Haine et al. 2015) and may mitigate the consequences of atlantification. However, we do observe that atlantification is extending far beyond the

https://doi.org/10.5194/egusphere-2025-2316
Preprint. Discussion started: 28 May 2025

Lomonosov Ridge, into the Makarov Basin of the Arctic Ocean with potentially profound implications for the regional ecological system (e.g., Polyakov et al. 2025a). Monitoring the fate of atlantification and understanding its role in climate change has great scientific and societal relevance, as this serves as a foundation for developing reliable forecasts and decision-making.

Acknowledgements. IVP acknowledges funding from Office of Naval Research Grant N00014-21-1-2577. IVP and AVP were supported by National Science Foundation (NSF) grant #1724523 and the U.S. Department of Energy grant 280253. LEK and MAC were supported by NSF grant numbers 2031853 and 2031854. KHC, JY, and EJY were supported by Korea Institute of Marine Science & Technology Promotion (KIMST) grant funded by the Ministry of Oceans and Fisheries (KIMST RS-2021-KS211500, Korea-Arctic Ocean Warming and Response of Ecosystem, KOPRI).

Competing interests: The authors declare that they have no conflict of interest.

Author Contributions. All authors participated in preliminary analysis; AP and IP carried out processing and analysis of mooring data, LK, MC, SD, JH and EC contributed to interpretation of hydrographic data and formulating objectives of the study, KHC, JJ, and EJY provided processing and analysis of KOPRI data. All authors contributed to interpreting the data and writing the paper.

Author Information. The authors declare no competing interests. Correspondence and requests should be addressed to IP (ivpolyakov@alaska.edu).

Data Availability Statement. All mooring data used in this study are available at https://arcticdata.io/catalog/#view/arctic-data. The ERA5 reanalysis data is available from https://cds.climate.copernicus.eu/cdsapp#!/home. Sea ice concentration is available from https://www.ncdc.noaa.gov/oisst. Mooring data used in this study are available on the web, at https://arcticdata.io/catalog/#view/arctic-data.7792.4.

https://doi.org/10.5194/egusphere-2025-2316
Preprint. Discussion started: 28 May 2025

References

Armitage, T. W. K., Bacon, S., Ridout, A. L., Petty, A. A., Wolbach, S., and Tsamados, M.: Arctic Ocean surface geostrophic circulation 2003–2014, The Cryosphere, 11, 1767–1780, https://doi.org/10.5194/tc-11-1767-2017, 2017.

Bauch, D., Torres-Valdes, S., Polyakov, I., Novikhin, A., Dmitrenko, I., McKay, J., and Mix, A., 2014: Halocline water modification and along slope advection at the Laptev Sea continental margin, *Ocean Sci.*, 10, 141–154, 2014 www.ocean-sci.net/10/141/2014/ doi:10.5194/os-10-141-2014.

Brenner, S., Thomson, J., Rainville, L., Crews, L. and Lee, C. M. Wind-driven motions of the ocean mixed layer in the western Arctic. J. *Phys. Oceanogr*., 53, 1787-1804, doi: 10.1175/JPO-D-22-0112.1, 2023.

Carmack, E. C., Yamamoto-Kawai, M., Haine, T. W. N., Bacon, S., Bluhm, B. A., Lique, C., Melling, H., Polyakov, I. V., Straneo, F., Timmermans, M.-L.: Fresh water and its role in the Arctic marine system: sources, delivery, disposition, storage, export, and physical and biogeochemical consequences in the Arctic and global oceans. *J. Geophys. Res. - Global Biogeochemical Cycles*. **121**, 675-717, doi:10.1002/2015JG003140/full, 2016.

Charette, M.A., Kipp, L.E., Jensen, L.T., Dabrowski, J.S., Whitmore, L.M., et al. The Transpolar Drift as a Source of Riverine and Shelf-Derived Trace Elements to the Central Arctic Ocean. J. Geophys. Res. Ocean. e2019JC015920. https://doi.org/10.1029/2019JC015920, 2020.

Ershova, E. A., and Kosobokova, K. N.: Cross-shelf structure and distribution of mesozooplankton communities in the East-Siberian Sea and the adjacent Arctic Ocean. *Polar Biol.* 42, 1353–1367. doi: 10.1007/s00300-019-02523-2, 2019.

Haine, T. W. N., B. Curry, R. Gerdes, E. Hansen, M. Karcher, C. Lee, B. Rudels, G. Spreen, L. de Steur, K. D. Stewart, R. Woodgate. Arctic Freshwater Export: Status, Mechanisms, and Prospects. *Global Planetary Change* **125**, 13-35. http:/dx.doi.org/10.1016 j.gloplacha.2014.11.013, 2015.

Jones, P. E. Circulation in the Arctic Ocean. *Polar Research,* 20(2), 139–146, 2001.

Kipp, L., M. Charette, A. Robbins, A. Pnyushkov, I. Polyakov, L. Whitmore: Radium isotops as tracers of shelf-basin exchange processes in the eastern Arctic Ocean. *J. Geophys. Res.: Oceans,* 128, e2023JC020303, https://doi.org/10.1029/2023JC020303, 2023.

https://doi.org/10.5194/egusphere-2025-2316
Preprint. Discussion started: 28 May 2025

Lenn, Y.-D., Rippeth, T. P., Old, C. P., Bacon, S., Polyakov, I., Ivanov, V., & Hollemann, J. A.: Intermittent intense turbulent mixing under ice in the Arctic Halocline of the Laptev Self Sea. *Journal of Physical Oceanography*, *43*(3), 531–547. https://doi.org/10.1175/ 2010jpo4425.1, 2011.

Lenn, Y.-D., Wiles, P., Torres-Valdes, S., Abrahamsen, E., Rippeth, T., Simpson, J. H., et al.: Vertical mixing at intermediate depths in the Arctic boundary current. *Geophysical Research Letters*, *36*, L05601. https://doi.org/10.1029/2008GL036792, 2009.

Lincoln, B. J., Rippeth, T. P., Lenn, Y.-D., Timmermans, M. L., Williams, W. J., and Bacon, S.: Wind-driven mixing at intermediate depths in an ice-free Arctic Ocean. *Geophysical Research Letters*, *43*, 9749–9756. https://doi.org/10.1002/2016GL070454, 2016.

Lundberg, M., and I. V. Polyakov: Climate change drives evolution of thermohaline staircases in the Arctic Ocean. *J. Geophys. Res*. 130, e2024JC021538, https://doi.org/10.1029/2024JC021538, 2025.

Peralta-Ferriz, C., and Woodgate, R.: Seasonal and interannual variability of pan-Arctic surface mixed layer properties from 1979 to 2012 from hydrographic data, *Progress in Oceanography*, 134, 19-53, 2015.

Pnyushkov, A. V., Polyakov, I. V., Rember, R., Ivanov, V. V., Alkire, M. B., Ashik, I. M., Baumann, T. M., Alekseev, G. V., and Sundfjord, A.: Heat, salt, and volume transports in the eastern Eurasian Basin of the Arctic Ocean from 2 years of mooring observations, Ocean Sci., 14, 1349-1371, https://doi.org/10.5194/os-14-1349-2018, 2018.

Pnyushkov A. V., Polyakov I. V., Alekseev G. V., Ashik I. M., Baumann T. M., Carmack E. C., Ivanov V. V. and Rember R.: A Steady Regime of Volume and Heat Transports in the Eastern Arctic Ocean in the Early 21st Century. Front. Mar. Sci. 8:705608. doi: 10.3389/fmars.2021.705608, 2021.

Polyakov, I. V., T. P. Rippeth, I. Fer, T. M. Baumann, E. C. Carmack, V. V. Ivanov, M. Janout, L. Padman, A. V. Pnyushkov, and Rember, R.: Intensification of Near-Surface Currents and Shear in the Eastern Arctic Ocean. *Geophys. Res. Lett.,* 46, e2020GL089469. https://doi.org/10.1029/2020GL089469, 2020a.

Polyakov, I. V., T. P. Rippeth, I. Fer, M. B. Alkire, T. M. Baumann, E. C. Carmack, R. Ingvaldsen, V. V. Ivanov, M. Janout, S. Lind, L. Padman, A. V. Pnyushkov, Rember, R.: Weakening of cold halocline layer exposes sea ice to oceanic heat in the eastern Arctic Ocean, *J. Climate*. 33(18), 8107-8123, doi 10.1175/JCLI-D-19-0976.1, 2020b.

https://doi.org/10.5194/egusphere-2025-2316
Preprint. Discussion started: 28 May 2025

Polyakov, I. V., R. B. Ingvaldsen, A. V. Pnyushkov, U. S. Bhatt, F. A. Francic, M. Janout, R. Kwok, and Ø. Skagseth: Fluctuating Atlantic inflows modulate Arctic Atlantification. *Science, 381,* 972-979, doi: 10.1126/science.adh5158, 2023.

Polyakov, I. V., A. V. Pnyushkov, M. Charette, K.-H. Cho, J. Jung, L, Kipp, M. Muilwijk, L. Whitmore, E. J. Yang, and Yoo, J. : Atlantification advances into the Amerasian Basin of the Arctic Ocean, *Sci. Advances*, 11(8), eadq7580, 2025a.

Polyakov, I. V., Q. Ding, M. Holland, and Stroeve, J.: Variability of North Polar Ocean / ice system, Encyclopedia of Climate System Science. Submitted, 2025b.

Proshutinsky, A., R. Krishfield, J. M. Toole, M.-L. Timmermans, W. Williams, S. Zimmermann, M. Yamamoto-Kawai, T. W. K. Armitage, D. Dukhovskoy, E. Golubeva, G. E. Manucharyan, G. Platov, E. Watanabe, T. Kikuchi, S. Nishino, M. Itoh, S.-H. Kang, K.-H. Cho, K. Tateyama, J. Zhao: Analysis of the Beaufort Gyre Freshwater Content in 2003–2018. *J. Geophys. Res.* **124**, 9658-9689, 2019.

Rainville, L., and Woodgate, R. A.: Observations of internal wave generation in the seasonally ice-free Arctic. *Geophysical Research Letters*, *36*, L23604. https://doi.org/10.1029/2009GL041291, 2009.

Stroeve, J., Notz, D.: Changing state of Arctic sea ice across all seasons. Environ. Res. Lett., 13, 103001, https://doi.org/10.1088/1748-9326/aade56, 2018.

Thurnherr, A.M., Goszczko, I., and Bahr, F.: Improving LADCP Velocity with External Heading, Pitch, and Roll, *J. Atmos. Oceanic Technol.,* 34, 1713–1721, https://doi.org/10.1175/JTECH-D-16-0258.1, 2017.

Timmermans, M.-L., J. M. Toole, The Arctic Ocean's Beaufort Gyre, *Annual Rev. Mar. Sci.*, 15, 223-248, https://doi.org/10.1146/annurev-marine-032122-012034, 2023.

Timmermans, M.-L., and Marshall, J.: Understanding the Arctic Ocean circulation: A review of ocean dynamics in a changing climate. *J. Geophys. Res.: Ocean*, 125(4), 1-35 https://doi.org/10.1029/2018JC014378, 2020.